Gas-Fluidization Characteristics of Binary Mixtures of Particles in 2D Geometry

Antonio Busciglio[*]   Giuseppa Vella[†]

Dr. G. Micale[‡]

[*]Università degli Studi di Palermo,
antonio.busciglio@unipa.it

[†]Università degli Studi di Palermo, giuseppa.vella@unipa.it

[‡]giorgiod.maria.micale@unipa.it

Gas-Fluidization Characteristics of Binary Mixtures of Particles in 2D Geometry

Antonio Busciglio, Giuseppa Vella, and Dr. G. Micale

Abstract

The bubbling behaviour of fluidized beds has been thoroughly investigated in the last decades by means of several techniques, e.g. X-ray, Inductance, Resistance and Impedance based techniques, PIV. In recent years, Digital Image Analysis Techniques have shown their potential for accurate and cost effectively measurements.

Most of the work related to bubble behaviour analysis deals with single-sized particles, while almost all industrial equipment operates with multi-sized particles. Although considerable work has been done in the past with focus on the analysis of the mixing-segregation behaviour and predictions of fluid dynamics regime transitions, a lack of knowledge still exists in the analysis of bubbles properties measurements for the case of polydispersed systems.

In this work, digital image analysis has been adopted to accurately measure fundamental global parameters such as bubble hold up and bed expansion as well as average bubble hold-up distribution maps or bubble size distributions in bubbling fluidized beds of binary mixtures of particles. The experiments have been carried out at steady state conditions with binary mixtures of corundum particles, at various inlet gas velocities. This preliminary study has been performed with the aim to collect valuable data for future development of predictive models and validation of CFD codes.

1. INTRODUCTION

In recent years, thanks to the continuous development of digital imaging systems and digital image processing, a great number of researchers have chosen digital visual methods to be applied in the field of experimental fluid dynamics, Lim et al. (2007), Mudde et al. (1994), Gera and Gautam (1995), Boemer et al. (1998), Hull et al. (1999), Shen et al. (2004), Busciglio et al. (2008). These techniques play a fundamental role in analysis and data acquisition for multiphase flows, where the observation of inter-phase boundaries is relatively simple. Digital visual methods are limited of course to the case of two-dimensional fluidized beds, as in this case bubbles can be easily observed. These methods result in non-invasive, cost saving and accurate measurements of bubble properties in fluidized beds. Because of the possibility of measuring statically significant number of bubbles, full statistical analysis can be easily performed.

It is worth noting that most of the work related to bubble behaviour analysis is concerned with single-sized particles, while almost all industrial equipment operates with broad distributions of particle size because of attrition and impact phenomena that broaden the initial particle size distribution. Several works are available in order to characterize the behaviour of solid particles mixtures when fluidized (Formisani et al., 2001; Marzocchella et al., 2000). The great part of these works are therefore related to the incipient fluidization behaviors, i.e. the development of correlation able to predict the minimum fluidization velocity for mixtures of particles (Ellis et al., 2004; Gauthier et al., 1999; Joaquin et al., 2000) or in characterizing the mixing/segregation characteristics of mixtures during the fluidization experiments (Bokkers et al., 2004). No experimental works were found for the characterization of bubbles rising up in mixtures of particles having different sizes or densities.

Some computational works have been found concerning the bubbles behavior in mixtures of particles having different sizes or densities. In particular, Owoyemi et al. (2008), presented a model for the prediction of the fluid dynamic behavior of binary suspensions of solid particles fluidized by Newtonian fluids. Predictions of the fluidization behavior obtained by the proposed model are validated against experimental results in terms of solid mixing and segregation, bed expansion and bubble dynamics. In another paper, Owoyemi et al., (2007), presented the validation of the same model for the simulation of bidispersed fluidized suspensions. Results are presented on the experimental and numerical investigation into the mixing and segregation behavior of a bidispersed fluidized mixture of natural rutile (flotsam) and slag (jetsam), which differ in size and having the same density. Computational results obtained for mixing and segregation patterns, bed expansion, and bubble dynamics are validated against experimental data.

On the basis of this lack of knowledge, the aim of the present work is to employ the Digital Image Analysis Technique by Busciglio et al., (2008) for investigating some of the essential features of fluidized binary mixtures of particles.

2. EXPERIMENTAL APPARATUS AND METHODS

Two different fluid-bed reactors were adopted for the present investigation. The first one is entirely made of Perspex with dimensions equal to 800(h)×180(width)×15(depth)mm. Front wall is made of glass in order to avoid Perspex® surface opacity due to particles attrition phenomena. The second reactor is made of aluminium and equipped with glass walls at front and back with dimensions equal to 1200(height × 240(width) × 10(depth)mm. Both reactors are therefore almost two-dimensional, to allow visual observation of bubble dynamics within the bed. A sintered plastic porous distributor (average particle diameter 150μm, average porosity equal to 0.35 determined by SEM analysis), with thickness equal to 10mm, is placed at the bottom of the particle bed. The measured pressure drop along the distributor is in accordance with the well accepted Ergun equation for porous media, Bird et al., (2002). Below the distributor a wind box filled with large glass particles (2−5mm) allows to fully equalize the gas flow. Air was used as fluidizing gas, its flow rate being accurately measured through a set of four flow-meters, within the range 0−140 lt/min. Four different kinds of particulates were used for the experimental runs: glass particles with density equal to 2500kg/m^3 of two different sizes, (i) 212−250μm hereafter referred to as flotsam particles and (ii) 500−600μm hereafter referred to as jetsam particles; corundum particles with density equal to 4000kg/m^3 of two different sizes, (iii) 212−250μm hereafter referred to as flotsam particles and (iv) 500−600 μm hereafter referred to as jetsam particles. The values of U_{mf} were experimentally determined for pure components, and found equal to 5.24cm/s, 28.7cm/s, 9.5cm/s and 40.1cm/s respectively. Moreover, the bubbling behavior of some corundum mixtures were investigated. The particles were filled up to a bed height of twice the bed width. For particle mixtures, the initial filling of the bed is made by two separate (unmixed) layers of particles. The $U_{mf,mix}$ value was estimated by means of literature correlations (Yang 2003) reported below:

$$d_m = \frac{X}{d_{p,flot}} + \frac{1-X}{d_{p,jet}}$$

(eq.1)

$$Ar = \frac{gd_m^{\,3}(\rho_p - \rho_g)\rho_g}{\mu_g^{\,2}} \qquad\qquad (eq.2)$$

$$\mathrm{Re}_{mf,mix} = \frac{\rho_g d_m U_{mf,mix}}{\mu_g} = 0.0054\,Ar^{0.78} \qquad\qquad (eq.3)$$

Five corundum mixtures were fluidized having composition X = 20%, X = 40%, X = 50%, X = 60%, X = 80% and (w/w) in the flotsam component. In the case of particle mixtures, the definition of minimum fluidization velocity is more troublesome, because of the onset of different behaviors such as partial de-fluidization, segregation and so on, that are strongly dependent on experimental conditions adopted. In the cases investigated, the bed was always operated at inlet gas velocities able to guarantee a fully fluidized state and homogeneous composition along the bed height. The minimum fluidization velocity estimated by means of Eqn.3 is therefore adopted only as a reference velocity. Experimental data were acquired after the achievement of full steady state, in order to avoid measuring bubble behavior during the initial mixing of powders. In this work, the observation was focused on the whole bed, without selecting any particular region of interest, to allow a full field analysis of the bubbling fluidization dynamics.

The bubble-related flow structures were visualized with the aid of a back-lighting device and recorded by a digital camcorder (mvBlueFox 121c), placed opposite to the bed at a distance of 270cm. Continuous high intensity uniform illumination was obtained by placing six fluorescent lamps at the back side of the bed, at approximately 10cm. A suitable system of fluorescent lamps was found to be best suited for bubble measurement, to avoid non-uniform illumination when high image acquisition rates are used (up to 50fps). The digital visual acquisition system allowed to collect images of the bed at different frequencies, ranging from 1Hz to 60Hz. Each experimental acquisition provides at least 500 frames. The image processing routine was developed on Matlab 7.3 (The MathWorks inc.). Full details on the image analysis technique are given elsewhere, Busciglio et al. (2008). The image analysis technique here adopted is able to obtain a very large amount of raw data about bubble properties inside the bed, that can be further post-processed to get concise and effective quantities for the assessment fluidized bed behavior.

3. RESULTS AND DISCUSSION

In this section, the data obtained will be discussed in detail, together with the numerical and statistical methods adopted for translation of large amount of raw data into information useful for fluidization quality characterization.

3.1 OVERALL BED CHARACTERIZATION

Bed expansion and overall bubble content within the bed are the easiest measure to take by means of image analysis (Busciglio et al.; 2008). It must be observed that the bed expansion dynamic and the relevant bubble hold-up dynamic, even if similar, represent rather different phenomena. In fact, overall bed expansion depends on both the extent of the bubble phase content and the average expansion of the emulsion phase (including, for example small non-visible bubbles, and the expanded cloud region), while bubble hold-up measures just bubbles overall content in the bed.

In Fig.1, an example of bed height and bubble hold up instantaneous values as a function of time are reported.
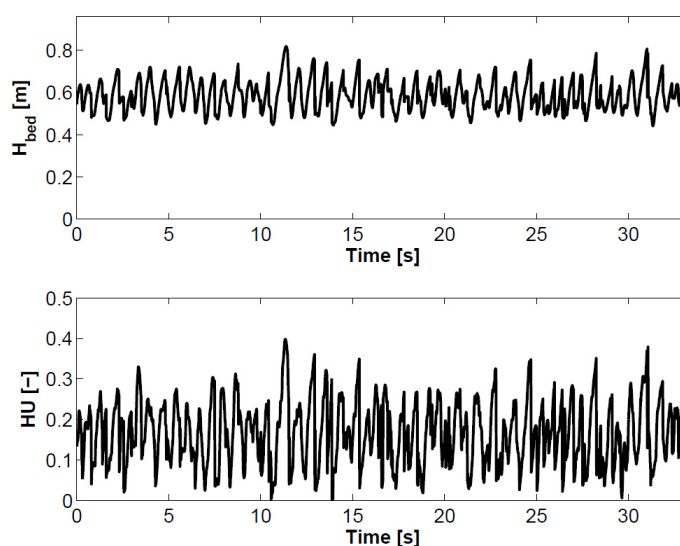

Figure 1. Example of instantaneous bed height and relevant bubble hold up as a function of time (Corundum mixture, $X = 0.5$, $U = 0.56 \text{m/s}$).

Once instantaneous values are obtained, time averaged data are readily obtained. A more convenient description of this "fluctuating" data can be obtained by the analysis of both mean values and relevant standard deviations (eventually normalized by the mean value), this latter being a good index of the fluctuation strength. In particular, the mean value of bed expansion (i.e. the ratio between the mean bed height $\mu(H_{bed})$ and the settled bed height H_0) and the relevant normalized standard deviation (i.e. the ratio between standard deviation of bed height $\sigma(H_{bed})$ and the relevant mean value $\mu(H_{bed})$) were computed for each case, the latter being a statistical measure of bed height fluctuations. The same quantities were computed for the case of average bubble hold up. All measured

data were conveniently reported in Fig.2 as a function of the excess gas velocity U-$U_{mf.}$.

In general, if the original two phase theory is assumed to be valid, a linear increase of bed expansion would be expected with increasing excess gas velocity, while more complex power-law dependence is expected if gas throughflow is accounted for (Geldart, 1967), or bubble growth due to coalescence is considered (Xavier et al., 1978, Geldart 1975). Anyway, a power law dependence on excess gas velocity is generally adopted in literature (Geldart, 1967) for the average bed expansion. The analysis of data reported in Fig.2 show that for each data series (same particles and geometry, different inlet gas velocity), both mean expansion and relevant standard deviation increase linearly.
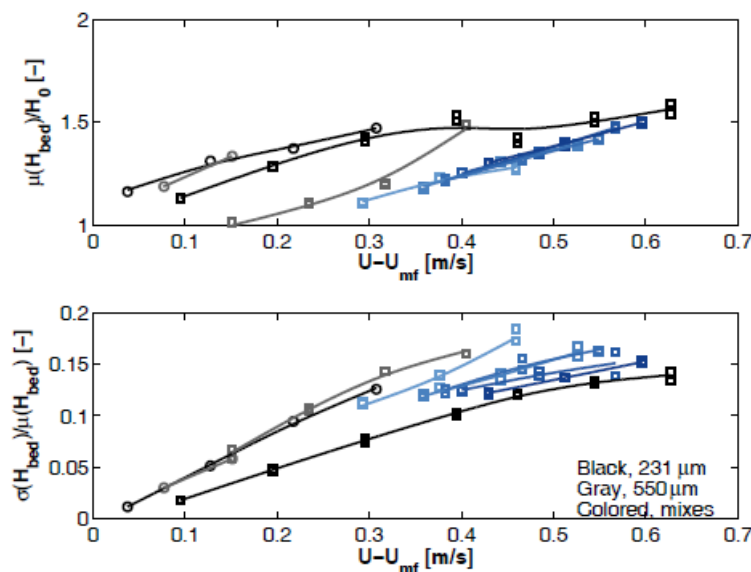

Figure 2. Bed expansion average values together with relevant standard deviations as a function of excess gas velocity. Circles refers to glass particles, squares to corundum particles. Mixes are indicated in a darker color the larger the content of flotsam component.

Notably, the mean expansion variation with excess gas velocity appears to be grouped in three different trends: (i) single-sized glass particles, showing the larger increment of bed expansion with excess gas velocity, with small difference of expansion at the same inlet gas velocity and different particle size; (ii) single-sized corundum particles, showing a quite similar expansion that of glass particles in the case of finer particles and a considerably smaller expansion in the case of coarser particles; (iii) corundum particle mixtures of two different sizes (iii and iv), that show an average expansion even lower than pure corundum particles. This last evidence is probably due to the fact that the initial filling of the bed was performed with separate particle layers of flotsam and jetsam particles. As a result a larger mean value of bed voidage is found with respect to perfectly mixed

condition of differently sized particles. Notably, the different behavior between glass particles (whose expansion value weakly depends on particle size) and corundum particles (whose expansion strongly decrease with increasing particle size) can be probably ascribed to the change of particle behavior according to Geldart's classification: in practice the coarser and denser corundum particles appear to behave as Geldart's D particles, while the finer and lighter glass particles appear to fluidize as Geldart's B particles in fast fluidization regime. These different characteristics change the gas throughflow and hence the functional dependence of bed expansion on excess gas velocity, although additional experimental work would be required in order to unambiguously assess the effect gas velocity on bed expansion. The analysis of standard deviations reported in the lower part of Fig.2 indicates a slightly different behavior: all the reported experimental data series show a linear trend with excess gas velocity that eventually approaches a constant value at the highest velocities. Notably, glass particles are characterized by the highest standard deviation values, regardless of the particle size, while corundum particles standard deviations strongly depend on the powder composition. In this case, the mixtures behavior is intermediate to that of mono-sized particles. Notably, for each data series (constant composition, varying gas velocity) it is possible to observe that an increase in the flotsam content (from pure jetsam to pure flotsam) leads to a decrease in the curve steepness. This is apparently counterintuitive, because the smaller the average particle size, the stronger the bubbling would be expected, because of the formation (and the consequent eruption) of larger bubbles. It will be shown in subsequent sections that this behavior is expected if a regime transition starts to occur. The analysis of bubble hold up average data and relevant standard deviations, reported in Fig.3 show that for excess gas velocities smaller than 0.3m/s, the average bubble hold up increases linearly with excess gas velocity with slope dependent only on particle diameter.

    For higher excess gas velocities, increasing linear trends are observed again with inlet gas velocity, with decreasing slope when passing from pure jetsam to pure flotsam particles. The standard deviation values, on the other hand, follow the same (qualitative) trend of bed height normalized standard deviation. On overall, it is possible to observe that a smooth transition generally occurs when passing from pure jetsam to pure flotsam particles, with the exception of mean bed expansion data. In fact, for each fixed composition, a linear trend of bed height standard deviation is found whose slope depends on powder composition only.
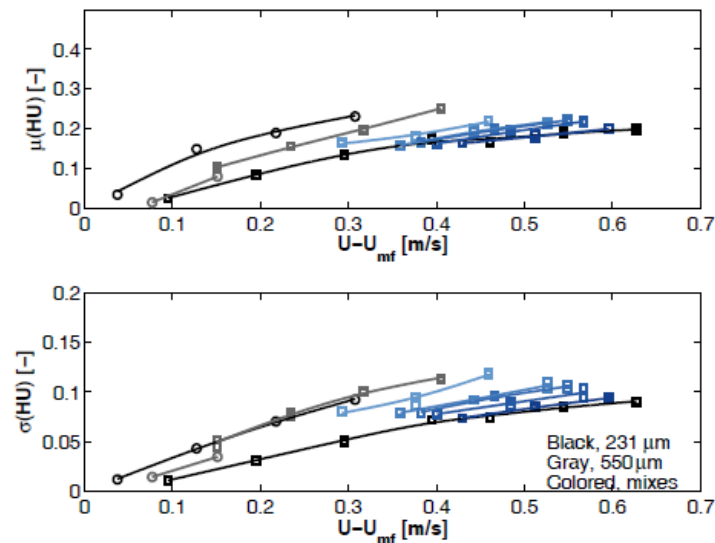
Figure 3. Overall bubble hold up average values together with relevant standard deviations as a function of excess gas velocity. Circles refers to glass particles, squares to corundum particles. Mixes are indicated in a darker color the larger the content of flotsam component.

3.2 LOCAL HOLD-UP MAPS

It has been already shown in a previous work (Busciglio et al., 2008) that averaged hold up maps can be simply obtained from binarized images of the fluidized bed taken with back-light technique. The distribution of bubbles in the bed is far from uniform. In cylindrical fluid beds, an annulus structure with the bubbles concentrated toward the walls of the vessel is formed close to the distributor (Werther and Molerus, 1973). Bubbles rising through the bed tend to migrate toward its center. As a consequence, the annular region of high bubble concentration decreases in diameter at higher elevations above the distributor, until it reaches the center of the vessel, provided that the bed is sufficiently tall. This last condition could lead to slug formation in upper regions of the bed. In this case, the solid particles transported upward by rising bubbles move downwards in the proximity of the vessel walls. On the contrary, if the bed is not sufficiently tall for a single slug chain to form, then solids transported upwards by bubbles return to the bottom of the bed moving downwards near the vessel walls and through the center of the bed, indicating that the final stage of bubble distribution development is not achieved. Similar results are reported for the case of 2-D fluidized beds (Lim et al., 2007) in which a pair of narrow bands of high concentration of bubbles along either sides of the bed close to the walls near the distributor is found. Bubbles gradually migrated inwards, spreading over the center of the bed towards the higher section of it. The authors claimed that the onset of this characteristic preferential path is mainly due to wall-constrained

motion of bubbles. Subsequent works (Lim et al., 2009; Shen et al., 2004) substantially confirm such findings. The average holdup maps reported in Figs. 4-6 show a bubble behavior that is qualitatively in good agreement with the observation and findings of Lim et al. (2007). The tapering of bubble distribution also leaves the regions close to the wall in the upper part of the bed deprived of bubbles. It is worth noting that the bed height at which the lateral bands reach the bed centerline gives indication of a fully developed bubbling regime.
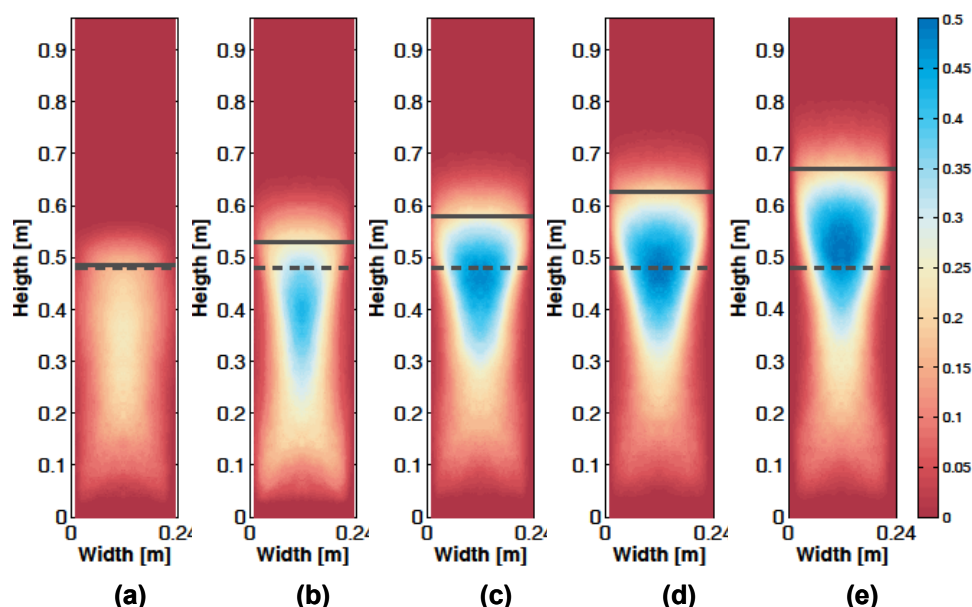

Figure 4. Local Bubble hold up maps at fixed inlet gas velocity (U = 0.56 m/s) and different flotsam compositions ((a) X = 0.0, (b) X = 0.2, (c) X = 0.5, (d) X = 0.8, (e) X = 1.0). The dashed lines show the bed height at rest, while the solid lines show the time averaged bed height.
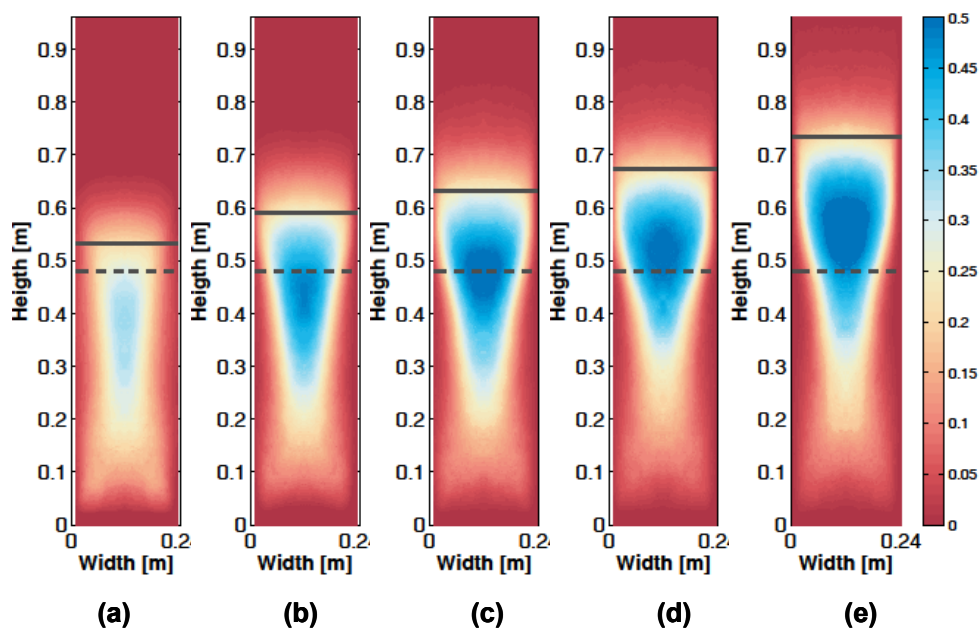
Figure 5. Local Bubble hold up maps at fixed inlet gas velocity (U = 0.64 m/s) and different flotsam compositions ((a) X = 0.0, (b) X = 0.2, (c) X = 0.5, (d) X = 0.8, (e) X = 1.0). The dashed lines show the bed height at rest, while the solid lines show the time averaged bed height.
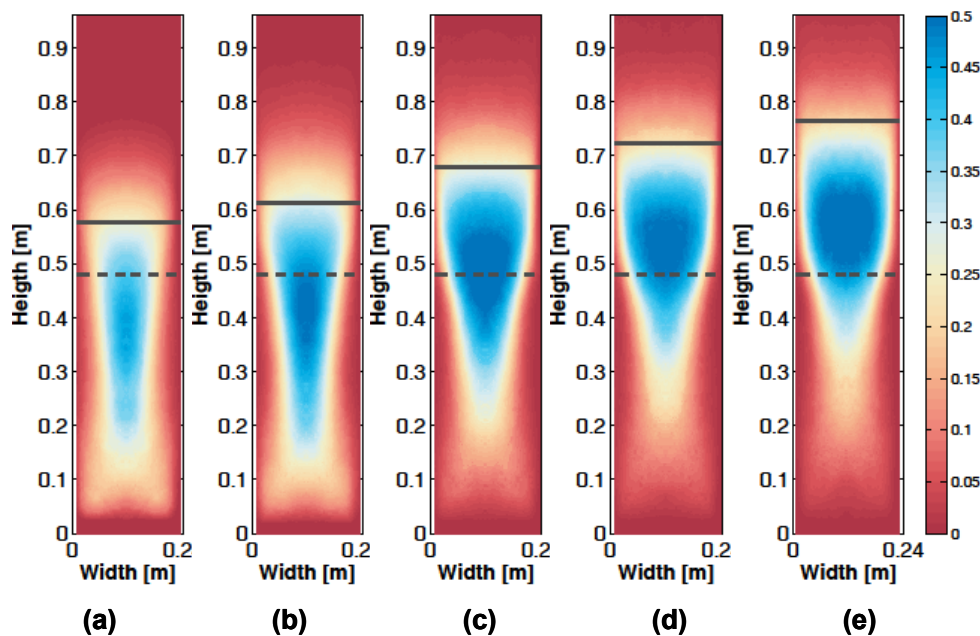

Figure 6. Local Bubble hold up maps at fixed inlet gas velocity (U = 0.72 m/s) and different flotsam compositions ((a) X = 0.0, (b) X = 0.2, (c) X = 0.5, (d) X = 0.8, (e) X = 1.0). The dashed lines show the bed height at rest, while the solid lines show the time averaged bed height.

Increasing inlet gas velocity, the tendency for bubbles to follow the reverse-Y path in the lower region of the bed increases, while the void distribution in the proximity of the bed surface appear to be increasingly occupied by the bubble phase, as it can be seen, for example in figure from 4.a to 4.e. When pure jetsam bed is considered (Figs. 4.a, 5.a, 6.a), the lateral band appear to reach the bed center very close to the distributor, below 0.2 m. In agreement with Lim et al. (2007) findings, near-wall zones in the proximity of the bed surface are almost bubble free. Conversely, when increasing flotsam content (for example, Figs.5.a 5.e), a rather different behavior is observed, the lateral bands of bubbles formed at the distributor reach the bed center at higher elevations, and a wide zone of high bubble content is formed on the whole bubble width. This kind of behavior can be likely to be due to the onset of constrained bubble growth and/or turbulent fluidization because of decrease of minimum fluidization velocity that in turn leads to an increase of excess gas velocity being the inlet gas velocity constant.

The analysis of time averaged hold-up maps is of course fully consistent with the bed height and bubble hold-up results previously presented in Figs.2-3.

3.3 BUBBLE SIZE

Some of the available experimental distributions of bubble equivalent diameters are reported as function of bubble distance from distributor. The full set of data are presented in Figs.7 and 8 for the case of corundum jetsam particles and mixtures respectively. The data are presented in raw cloudy form, in order to highlight the complex bubble behavior along bed height.
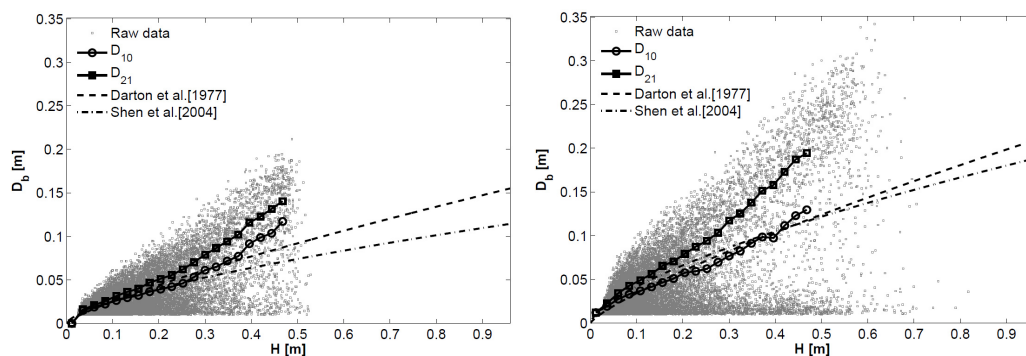

Figure 7. Bubble size evolution along bed height data at two different inlet gas velocities (right, u = 0.56 m/s; left, u = 0.72 m/s) for corundum particles (d_p = 550 μm), with average curves and relevant comparison with literature correlations.

In order to summarize data, one could try to adopt general averaged bubble sizes as a function of the distance above the distributor. Such locally averaged data are in general defined as:

$$D_{ij} = \frac{\sum D^i}{\sum D^j}$$
(eq.4)

In particular, the D10 value coincides with the arithmetic average, while it can be easily shown that the D21 value is proportional in 2-D beds to the ratio between overall bubble volume and surface. An average value is computed at each elevation above the distributor, provided that bubble position is unambiguously identified by the position of its centroid (Busciglio et al., 2008).

The average curves reported in Fig.7 only gives a rough description of the data trend shown. Conversely, the cloudy data presented allow the visualization of the small bubbles that are inside the bed even at the highest elevations, while an average curve could not show such characteristic and complexity. However, the presence of a wide distribution of bubble sizes is evident at all elevations of the bed, as a result of the splitting and/or nucleation phenomena. At increasing gas velocities, the increase in bubble diameter is more pronounced, as physically expected. Moreover, the presence of small bubbles in upper regions of the bed appear to be less pronounced with increasing velocity, due to the onset of slugs in such regions. This results are in agreement with the finding of Hulme and Kantzas (2004).

When corundum mixtures are considered, as reported in Fig.8, a considerably larger amount of small bubbles is evident at all elevations, but the average bubble size tends to increase with the excess gas velocity and elevation above the distributor.
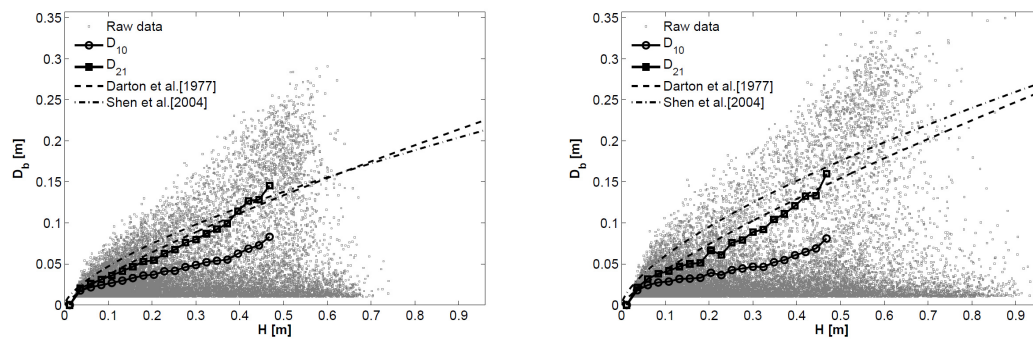

Figure 8 Bubble size evolution along bed height data at two different inlet gas velocities (right, u = 0.56 m/s; left, u = 0.72 m/s) for corundum particles (mixture at 50% flotsam content), with average curves and relevant comparison with literature correlations.

The data, obtained for two different corundum mixtures, assume the form of a wide cloud, but the number of small bubbles is much larger at all elevations with respect to the data reported in Fig.7. This fact is due to the high inlet gas velocities adopted for these experiments (the inlet gas velocity must overcome the final fluidization velocity of the mixture U_{ff} to guarantee the homogeneous composition of the bed), that leads to very strong bubbling conditions, especially in the upper section of the bed. This regime leads to the strong presence of small shrank bubbles at all elevations, as also reported by Hulme and Kantzas, (2004). This in turn leads to a decrease of the average diameter curve slope when increasing the inlet gas velocity.

A different way for bubbling characterization passes through the analysis of the overall bubble size distribution (BSD). Some experimental distributions of bubble equivalent size distribution on the whole bed are reported in Fig.9. The experimental distributions show a characteristic positive skewness of the distributions at all inlet gas velocities, in accordance with relevant literature data, (Argyriou et al., 1971; Morooka et al., 1972; Werther and Molerus 1974a, 1974b; Rowe and Yacono, 1975; Agarwal, 1985; Lim and Agarwal; 1990, Liu and Clark, 1995; VanLare et al., 1997).
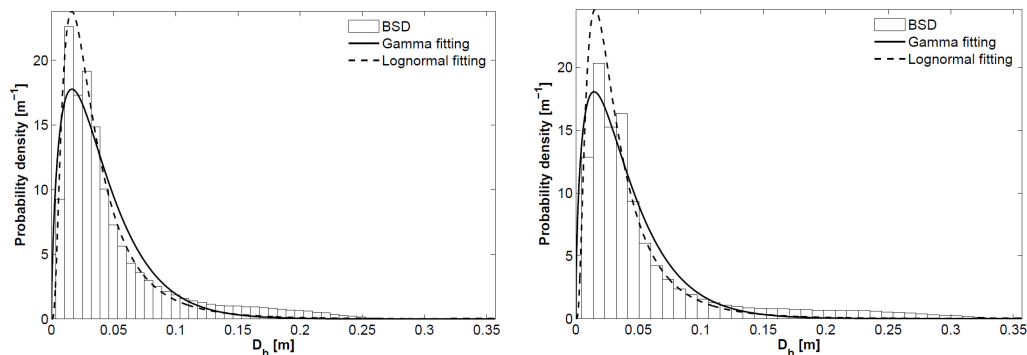

Figure 9. Bubble size distribution data on the whole bed at two different inlet gas velocities (right, u = 0.56 m/s; left, u = 0.72 m/s) for corundum particles (mixture at 50% flotsam content), together with fitted parametric distributions.

Two parametric distributions were adopted for the fitting of experimentally measured BSD, as suggested in several literature works: (i) the Gamma distribution (Eqn. 5; Argyriou et al., 1971; Morooka et al., 1972; Rowe and Yacono, 1975; Liu and Clark, 1995) and (ii) the Log-normal distribution (Eqn. 6 Werther et al., 1974a; VanLare et al., 1997). The fitted distributions were reported together with experimental BSDs in Fig.9.

$$BSD_{gamma} = \frac{1}{G_2^{G_1}\Gamma(G_1)} D_b^{G_1-1} e^{-D_b/G_2}$$

(eq.5)

$$BSD_{logn} = \frac{1}{D_b L_2 \sqrt{2\pi}} e^{-\frac{(\ln D_b - L_1)^2}{2L_2^2}}$$

(eq.6)

It is worth noting that in general both distribution types acceptably describe experimental data with the exception of is right-hand tail, i.e. those describing the population of larger bubbles. This is likely to be due to the simultaneous presence of small bubbles (at all elevation above the distributor) and large bubbles (formed by coalescence of smaller bubbles). Notably, it is well expected that the number of small bubbles largely exceeds that of large bubbles: this in practice gives rise to the disagreement in BSD fitting shown in Fig.9. In fact, as discussed in previous section, for the case of mixed corundum particles a considerably larger amount of small bubbles is always present at all elevation, therefore partially hiding the large-bubble-related tail.

However, for a first-guess of bubble population, the adoption of BSD can be considered quite satisfactory. The best-fit parameters for the Gamma were reported in Fig.10 as a function of excess gas velocity, while best-fit parameters for the Lognormal distributions are reported in Fig.11:
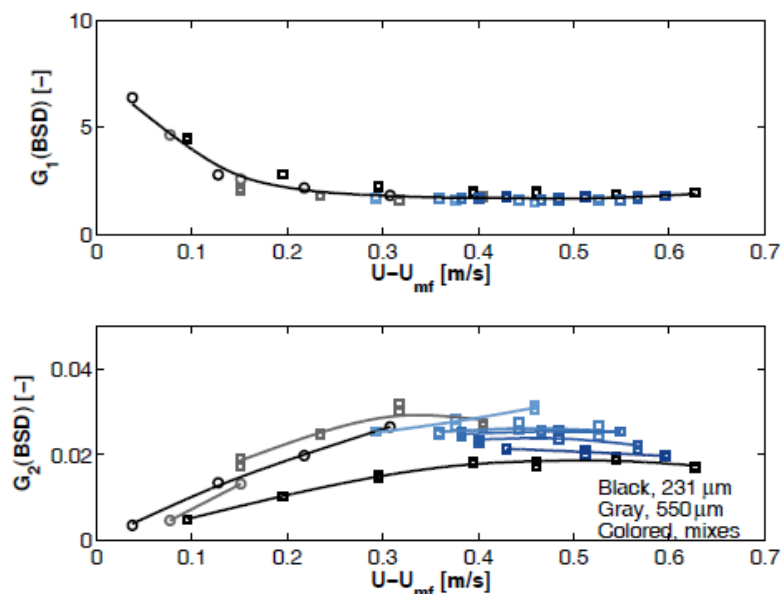

Figure 10. Gamma distribution parameters: circles, glass particles; squares, corundum particles. Mixes are indicated in a darker color the larger the content of flotsam component.

It is worth reminding that the Gamma distribution is a two parameter distribution in which the first parameter G_1 acts as a *shape* parameter, while the second parameter G_2 act as the *scale* parameter. Notably, the analysis of all data reported in Fig.10 points out that the smaller the excess gas velocity, the larger is the distribution shape parameter, and therefore, the distribution results more similar to a Gaussian (non-skewed) distribution. Conversely, at higher inlet gas velocities, an almost constant value of the shape parameter G_1 approx 2 is found. A quite different dependence on excess gas velocity is found analyzing the second distribution parameter, the scale parameter G_2: for each data series (constant composition and type of particles, varying inlet gas velocity), an increase of G_2 with excess gas flow is found, with a steeper dependence at the lowest excess gas velocities and almost constant values at the highest inlet gas velocities. This fact highlights that a wide range of bubbling behaviors is found in the experiments, ranging from normal bubbling to highly bubbling- fast bubbling regimes.
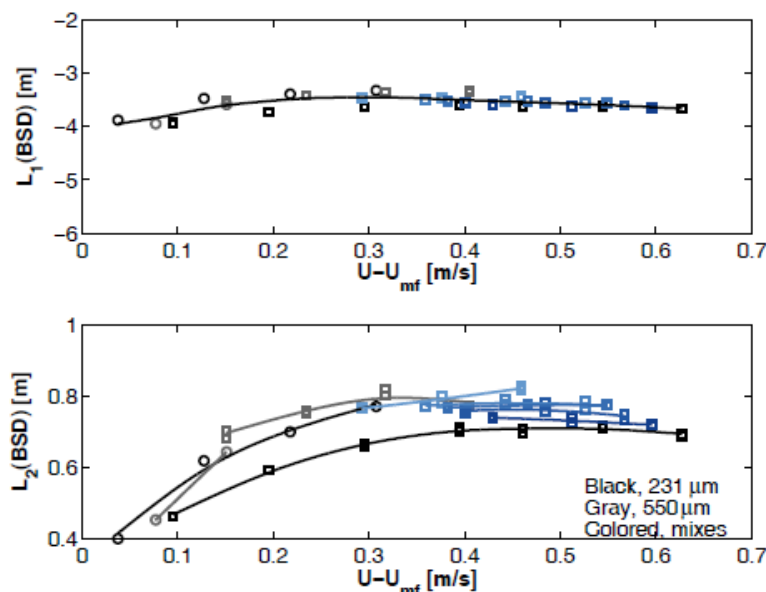

Figure 11. Lognormal distribution parameters: circles, glass particles; squares, corundum particles. Mixes are indicated in a darker color the larger the content of flotsam component.

A quite similar discussion applies to Fig.11: the first parameter represent the mean value of the logarithm of the bubble diameter sample under analysis, while the second parameter represent its relevant standard deviation. Notably, if the bed would exhibit a weak bubbling regime, the L_1 value will increase as well as the relevant L_2. This is shown in Fig.11 at the lowest inlet gas velocity, while

again, at the highest inlet gas velocities, almost constant values of L_1 and weakly dependent L_2 values on excess gas flow are reported.

This is of course justified if it is assumed that at the highest inlet gas velocities a re-arrangement of bubbly flow occurs with bubble break-up due to highly turbulent bubble motion and interactions. This in turn leads to the formation of a population of smaller bubbles at all elevations, as already seen and discussed in previous sections.

4. CONCLUSIONS

A thorough experimental study of overall fluidization characteristics in the case of mixed fluidized particles with same density and different sizes has been performed. The data so obtained highlight the complexity of phenomena involved. Several operating conditions were analyzed, widely varying the inlet gas velocity and the powder composition, this latter aspect being poorly analyzed in the pertinent literature. The analysis of bubbling dynamics of mixed powders has shown that most of the properties investigated can be sufficiently well explained on the basis of well accepted parameters such as the excess gas flow, provided that some care must be taken in data analysis when high velocity fluidization is considered.

REFERENCES

Agarwal, P.K., "Bubble charateristics in gas fluidized beds", Chemical Engineering Research and Design, 1985, 63, 323-337.

Argyriou, D.T. and List, H.L. and Shinnar, R., "Bubble Growth by Coalescence in Gas Fluidized Beds, AIChE Journal., 1971, 17, 122-130.

Bird, R., Stewart, W. and Lightfoot, E., "Transport Phenomena", Second Edition, 2002, Wiley, New York.

Boemer, A., Qi, H. and Renz, U., "Verification of Eulerian simulation of spontaneous bubble formation in a fluidized bed", Chemical Engineering Science, 1998, 1835-1846.

Bokkers G.A., van Sint Annaland M. and Kuipers J.A.M., "Mixing and segregation in a bidisperse gas–solid fluidised bed: a numerical and experimental study", Powder Technology, 2004, 140, 176–186.

Busciglio, A., Vella, G., Micale, G. and Rizzuti, R., "Analysis of the bubbling behaviour of 2-D gas solid fluidized beds. Part I. Digital image analysis technique", Chemical Engineering Journal, 2008, 140, 398–413.

Ellis, N., Bi, H.T., Lim C.J. and Grace, J.R., "Hydrodynamics of turbulent fluidized beds of different diameters", Powder Technology, 2004, 141, 124–136.

Formisani, B., Cristofaro, G. and Girimonte, R., "A fundamental approach to the phenomenology of fluidization of size segregating binary mixtures of solids", Chemical Engineering Science, 2001, 56, 109-119.

Gauthier, D., Zerguerras, S. and Flamant G., "Influence of the particle size distribution of powders on the velocities of minimum and complete fluidization", Chemical Engineering Journal, 1999, 74, 181-196.

Geldart, D., "Predicting the expansion of gas fluidized beds", "Fluidization Technology", 1975, 237-244, Hemisphere, Washington,

Geldart, D., "The expansion of bubbling fluidized beds" Powder Technology, 1967, 1, 355–368.

Gera, D. and Gautam, M., "Bubble rise velocity in two-dimensional fluidized beds", Powder Technology, 1995, 84, 283–285.

Hull, A.S., Chem, Z., Fritz, J.W. and Agarwal, P.K., "Influence of horizontal tube tanks on the behaviour of bubbling fluidized beds. 1. Bubble hydrodynamics", Powder Technology, 1999, 103, 230–242.

Hulme, I. and Kantzas, A., "Determination of bubble diameter and axial velocity for a polyethylene fluidized bed using X-ray fluoroscopy", Powder Technology, 1967, 147, 20–33.

Joaquin, R., Enrique, V. and Puigjaner, L., "Predicting the minimum fluidization velocity of polydisperse mixtures of scrap-wood particles", Powder Technology, 2004, 111, 245–251.

Lim, C.N. and Gilbertson, M.A. and Harrison, A.J.L., "Characterisation and control of bubbling behaviour in gas-solid fluidised beds, Control Engineering Practice, 2009, 17, 67-79.

Lim, C.N., Gilbertson M.A. and Harrison, A.J.L, "Bubble distribution and behaviour in bubbling fluidized beds", Chemical Engineering Science, 2007, 62, 56–69.

Lim, K.S. and Agarwal, P.K., "Conversion of pierced lengths measured at a probe to bubble size measures: an assessment of the geometrical probability approach and bubble shape models", Powder Technology, 1990, 63, 205-219.

Liu, W. and Clark, N.N., "Relationship between distributions of chord lengths and distribution of bubble sizes including their statistical parameters", International Journal of Multiphase Flow, 1995, 21, 6, 1073-1089.

Marzocchella, A., Salatino, P., Di Pastena, V. and Lirer L., "Transient Fluidization and Segregation of Binary Mixtures of Particles", AIChE Journal, 2000, 46, 2175–2182.

Morooka, S. and Tajima, K. and Miyauchi, T., "Behaviour of gas bubble in fluid beds", International Chemical Engineering., 1972, 12, 168-174.

Mudde, R., Schulte, H. and van der Akker, H., "Analysis of a bubbling 2-d gas-fluidized bed using image processing", Powder Technology, 1994, 81, 149–159.

Owoyemi, O. and Lettieri, P., "Computational Fluid Dynamics Modeling and Validation of Bidisperse Fluidized Industrial Powders", Industrial &. Engineering Chemistry Research, 2008, 47, 6316–6326.

Owoyemi, O., Mazzei, L. and Lettieri P., CFD modeling of binary-fluidized suspensions and investigation of role of particle-particle drag on mixing and segregation, AIChE Journal, 2007, 53, 1924-1940.

Rowe, P.N. and Yacono, C., "The distribution of Bubble Size in Gas Fluidized Beds, Transactions of the Institution of Chemical Engineers, 1975, 53, 59-60.

Shen, L., Johnsson, F. and Leckner, B., "Digital image analysis of hydrodynamics two-dimensional bubbling fluidized beds", Chemical Engineering Science, 2004, 59, 2607–2617.

van Lare, C.E.J. and Piepers, H.W. and Schoonderbeek, J.N. and Thoenes, D., "Investigation on bubble characteristics in a gas fluidized bed", Chemical Engineering Science, 1997, 52, 829-841.

Werther, J. and Molerus, O., "The local structure of gas fluidized beds-II. The spatial distribution of bubbles", International Journal. of Multiphase Flow, 1973, 1, 123-138

Werther, J., "Bubbles in Gas Fluidized Beds - Part I, Transactions of the Institution of Chemical Engineers, 1974a, 52, 149.

Werther, J., "Bubbles in Gas Fluidized Beds - Part II, Transactions of the Institution of Chemical Engineers, 1974b, 52, 160.

Xavier, A.M. and Lewis, D.A. and Davidson, J.F., "The expansion of bubbling fluidised beds", Transactions of the International Chemical Engineering, 1978, 56, 274-280.

Yang, W. C., "Handbook of fluidization and fluid particle systems", 2003, Marcel Dekker (Hemisphere), New York.